Journal of Geophysical Research

Supporting Information for

Predictability of the 2020 Antarctic strong vortex event and the role of ozone forcing

Eun-Pa Lim[1], Linjing Zhou[1], Griffith Young[1], S. Abhik[2], Irina Rudeva[1], Pandora Hope[1], Matthew C. Wheeler[1], Julie M. Arblaster[2], Harry H. Hendon[2], Gloria L. Manney[3,4], Seok-Woo Son[5], and Jiyoung Oh[6]

[1] Eun-Pa Lim1, Linjing Zhou1, Griffith Young1, S. Abhik2, Irina Rudeva1, Pandora Hope1, Matthew C. Wheeler1, Julie M. Arblaster3, Harry H. Hendon3, Gloria L. Manney4,5, Seok-Woo Son6, Jiyoung Oh7

[1] Bureau of Meteorology, Melbourne, Victoria, Australia

[2] School of Earth, Atmosphere and Environment, Monash University, Clayton, Victoria, Australia

[3] Securing Antarctica's Environmental Future, School of Earth, Atmosphere and Environment, Monash University, Clayton, Victoria, Australia

[4] NorthWest Research Associates, Socorro, New Mexico, USA

[5] Department of Physics, New Mexico Institute of Mining and Technology, Socorro, New Mexico, USA

[6] School of Earth and Environmental Sciences, Seoul National University, Seoul, Republic of Korea

[7] Korea Meteorological Administration, Seoul, Republic of Korea

Contents of this file

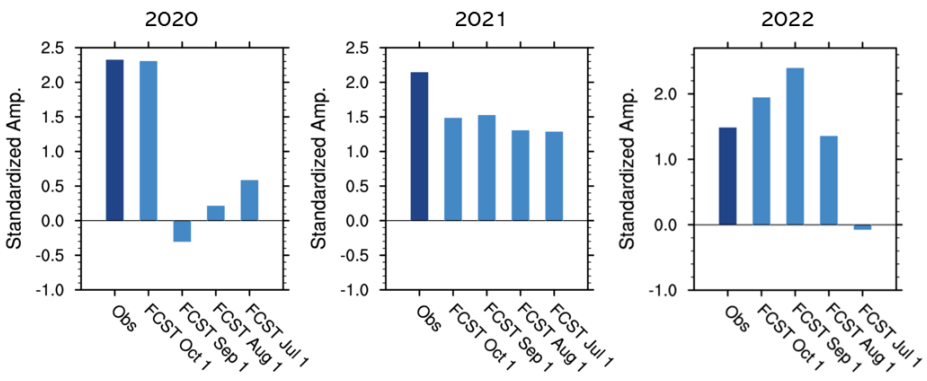

Figure S1. The Bureau of Meteorology (BoM)'s dynamical forecasts for the October-December mean stratospheric polar vortex of the SH ([U]' at 60°S, 10 hPa) for 2020, 2021 and 2022. The 2020 and 2021 events were predicted by ACCESS-S1 and the 2022 event was predicted by ACCESS-S2 because ACCESS-S2 became operational at the BoM in October 2021. The dark blue bars indicate the observed strengths of the vortices, and the light blue bars show the forecast strengths as a function of forecast start date as denoted on the x-axis. The observed and forecast standardized anomalies were obtained relative to their respective climatological means and standard deviations of 1990-2012 when ACCESS-S1 hindcasts are available. This figure shows that the 2021 and 2022 strong vortex events during the October-December season were predictable from the beginning of August (i.e., 2-month lead time), whereas the 2020 strong vortex event was only predictable from the beginning of October (i.e., zero lead time).

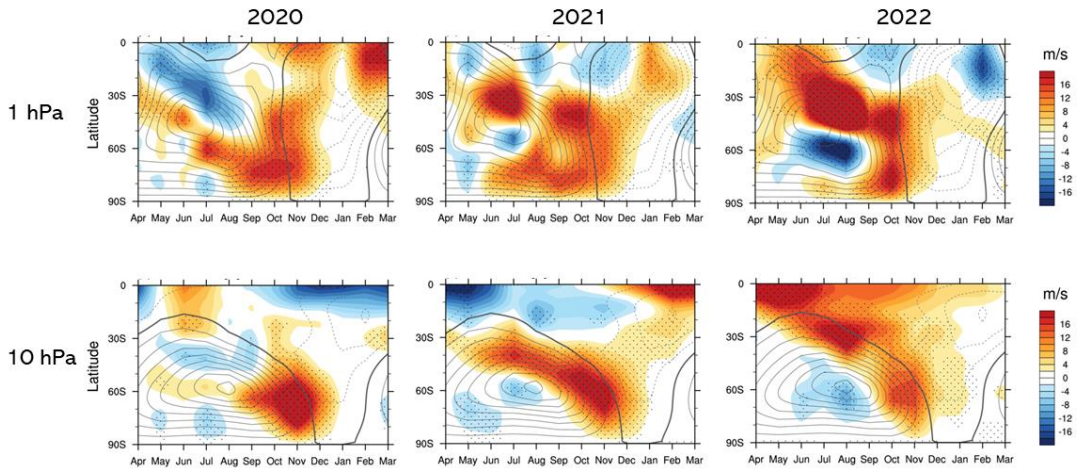

Figure S2. Zonal-mean zonal wind anomalies ([U]') at 1 hPa (upper panels) and 10 hPa (lower panels) for 2020, 2021 and 2022. Contours indicate the 1981-2018 climatologies of the zonal-mean zonal winds at the 1 and 10 hPa levels with 10 ms-1 intervals. Stippling indicates anomalies greater than 1 standard deviation estimated over the climatological period. The 2021 and 2022 strong vortex events over Antarctica observed from October to December at 10 hPa were associated with equatorward shifts of the winter stratospheric jet and subsequent poleward movements of increased westerly anomalies in the midlatitudes, which is consistent with the historical relationship of zonal-mean zonal wind anomalies associated with strong polar vortex events in 1981-2018 (main article Figure 3c). On the other hand, the winter to spring evolution of the 2020 strong vortex was different from those of the 2021 and 2022 events or that of the historical pattern.

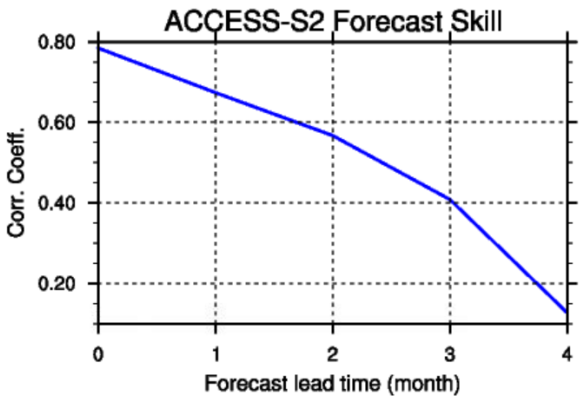

Figure S3. ACCESS-S2 hindcast (retrospective forecast) skill for the October-December mean stratospheric polar vortex of the SH monitored by [U]' at 60°S and 10 hPa. The 9-member ensemble mean forecasts as used in Wedd et al. (2022) were verified against the index derived from the JRA-55 reanalysis for 1981-2018. Correlation coefficients greater than 0.3 are statistically significant at the 95% confidence level, as assessed by a one-tailed student t-test given 38 samples.

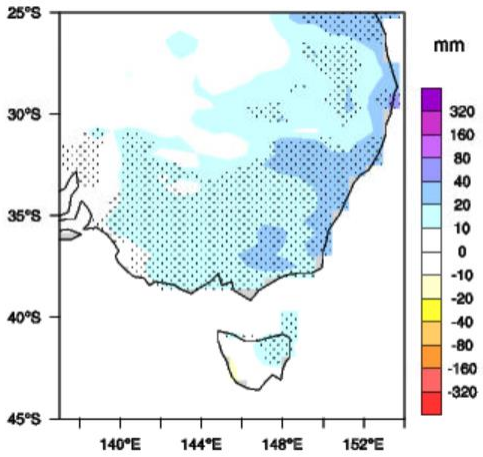

Figure S4. The rainfall and SAM relationship in December-January-February simulated in ACCESS-S2 hindcasts over 1981-2018 at 3-month lead time. The forecast SAM index was obtained by projecting the forecast 700-hPa geopotential height (GPH) anomaly data onto the pattern of the leading EOF mode of the observed variability of the 700-hPa GPH poleward of 20°S, which was derived using the JRA-55 reanalysis data and is displayed in Figure S5. Stippling indicates the statistical significance on the regression coefficients at the 90% confidence level, assessed by a two-tailed student t-test with 38 samples.

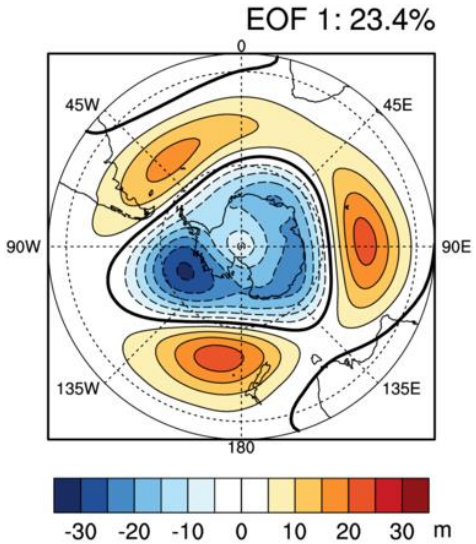

Figure S5. JRA-55 monthly 700-hPa GPH anomalies regressed onto the standardized time series of the 1st EOF mode of variability of monthly mean 700-hPa GPH, following (Thompson & Wallace, 2000). The EOF analysis was performed on the GPH anomalies weighted by squared cosine latitude over the domain of 20–90°S in the period of 1981–2018. The GPH anomaly pattern associated with the positive index polarity of the SAM is displayed, and the explained variance by this mode is shown in the top right corner of the figure.